JACS
JOURNAL OF THE AMERICAN CHEMICAL SOCIETY

Article

pubs.acs.org/JACS

Determination of Pre-Steady-State Rate Constants on the *Escherichia coli* Pyruvate Dehydrogenase Complex Reveals That Loop Movement Controls the Rate-Limiting Step

Anand Balakrishnan, Natalia S. Nemeria, Sumit Chakraborty, Lazaros Kakalis, and Frank Jordan*

Department of Chemistry, Rutgers the State University, Newark, New Jersey 07102, United States

Supporting Information

ABSTRACT: Spectroscopic identification and characterization of covalent and noncovalent intermediates on large enzyme complexes is an exciting and challenging area of modern enzymology. The *Escherichia coli* pyruvate dehydrogenase multienzyme complex (PDHc), consisting of multiple copies of enzymic components and coenzymes, performs the oxidative decarboxylation of pyruvate to acetyl-CoA and is central to carbon metabolism linking glycolysis to the Krebs cycle. On the basis of earlier studies, we hypothesized that the dynamic regions of the E1p component, which undergo a disorder−order transition upon substrate binding to thiamin diphosphate (ThDP), play a critical role in modulation of the catalytic cycle of PDHc. To test our hypothesis, we kinetically characterized ThDP-bound covalent intermediates on the E1p component, and the lipoamide-bound covalent intermediate on the E2p component in PDHc and in its variants with disrupted active-site loops. Our results suggest that formation of the first covalent predecarboxylation intermediate, C2α-lactylthiamin diphosphate (LThDP), is rate limiting for the series of steps culminating in acetyl-CoA formation. Substitutions in the active center loops produced variants with up to 900-fold lower rates of formation of the LThDP, demonstrating that these perturbations directly affected covalent catalysis. This rate was rescued by up to 5-fold upon assembly to PDHc of the E401K variant. The E1p loop dynamics control covalent catalysis with ThDP and are modulated by PDHc assembly, presumably by selection of catalytically competent loop conformations. This mechanism could be a general feature of 2-oxoacid dehydrogenase complexes because such interfacial dynamic regions are highly conserved.

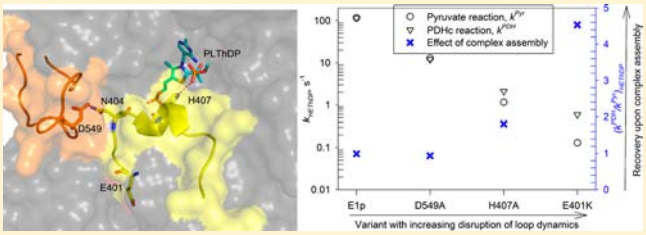

INTRODUCTION

The pyruvate dehydrogenase multienzyme complex from *Escherichia coli* (PDHc) is a 4500 kDa molecular machine, a member of the superfamily of enzymes that catalyze oxidative decarboxylation of 2-oxoacids, generating the corresponding acyl-Coenzyme A and NADH. The complex catalyzes the oxidative decarboxylation of pyruvate according to the overall reaction in eq 1:[1]

$$\text{pyruvate} + \text{CoA} + \text{NAD}^+ \rightarrow \text{acetyl-CoA} + \text{NADH} + \text{CO}_2 + \text{H}^+ \quad (1)$$

The PDHc is comprised of three enzyme components: (1) pyruvate dehydrogenase (E1p, EC 1.2.4.1) present in 24 copies with a mass of 99 474 Da; (2) dihydrolipoyl acetyltransferase (E2p, EC 2.3.1.12) also present in 24 copies with a mass of 65 959 Da; and (3) dihydrolipoyl dehydrogenase (E3p, EC 1.8.1.4) present in 12 copies with a mass of 50 554 Da.[2−4] The E1p component catalyzes thiamin diphosphate (ThDP)-dependent decarboxylation of pyruvate, whose product reductively acetylates the covalently bound lipoamide group on E2p. The acetyl group is then transferred from acetyldihydrolipoamide to Coenzyme A (CoA) bound at the catalytic domain of E2p, then dihydrolipoamide is reoxidized by a FAD group bound to the E3 component, while the resulting $FADH_2$ is reoxidized to FAD by NAD^+, finally producing NADH (Scheme 1A).

X-ray crystallographic studies on the E1p component, an α_2 homodimer, revealed a disorder-to-order transition of two dynamic loops of E1p spanning residues 401−413 (inner active center loop) and 541−557 (outer active center loop) seen only in the presence of a stable predecarboxylation intermediate analogue C2-α-phosphonolactylThDP (PLThDP) in the active site.[5] The intermediate analogue interacts with a conserved histidine residue His407, thus ordering the inner loop, and interaction between residues Asn404 and Asp549 further orders the outer loop over the active site, thus forming a new surface during the life of the closed state (Figure 1). In the H407A E1p variant, binding and reductive acetylation of E2p lipoyl domains were highly impaired, suggesting an important role in steps leading to transfer of acetyl moiety from the E1p active site to the lipoyl group on E2p.[6] In addition, extensive biochemical and biophysical studies by Kale et al. using inner loop variants by substitutions at charged residues showed that the disorder-to-order transition is essential for substrate entry and to sequester the E1p active sites to prevent undesirable side reactions.[7] EPR studies using a nitroxide label introduced into

Received: June 26, 2012
Published: October 22, 2012

   dx.doi.org/10.1021/ja3062375 | J. Am. Chem. Soc. 2012, 134, 18644−18655

Scheme 1. (A) Mechanism of *E. coli* Pyruvate Dehydrogenase Complex with Role of ThDP on E1p; and (B) Oxidation of Enamine by DCPIP

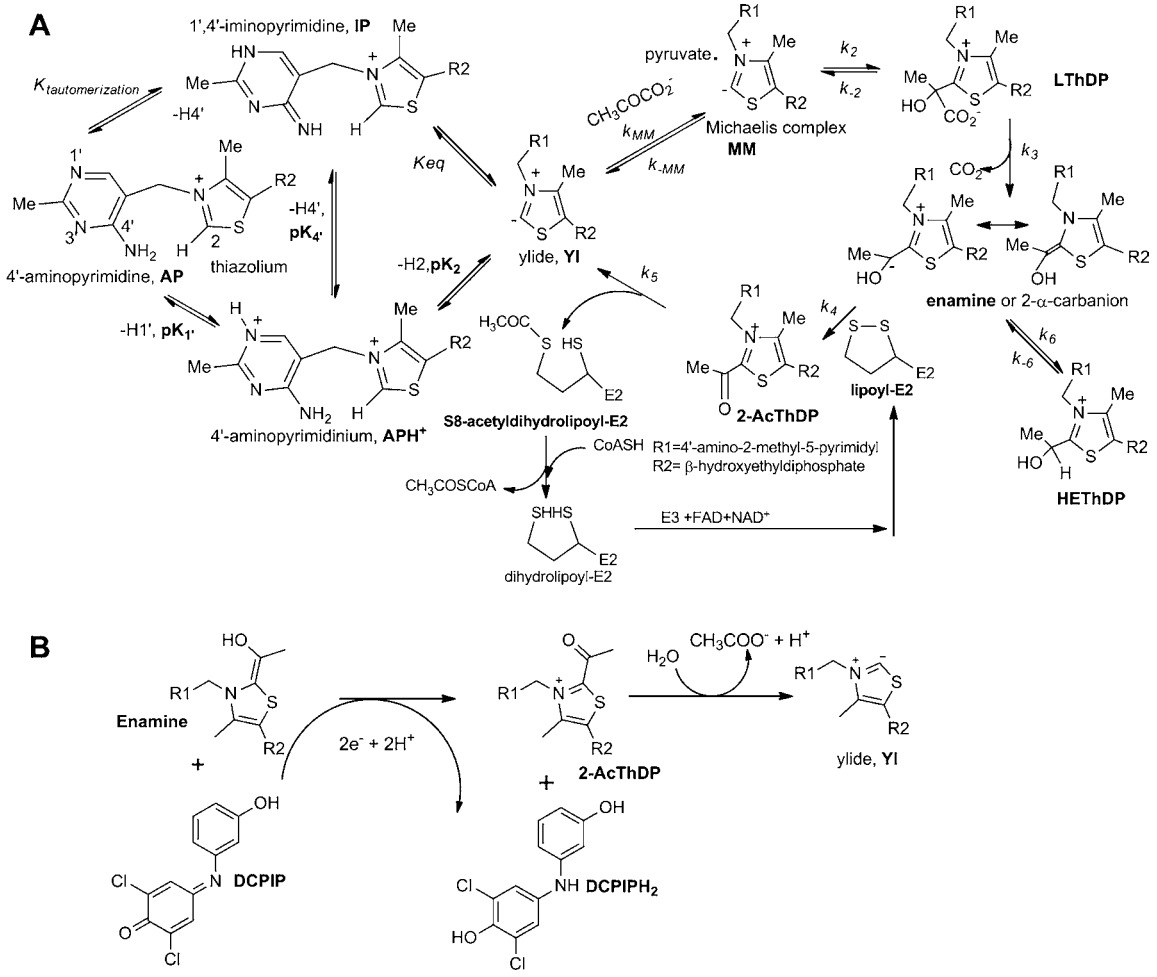

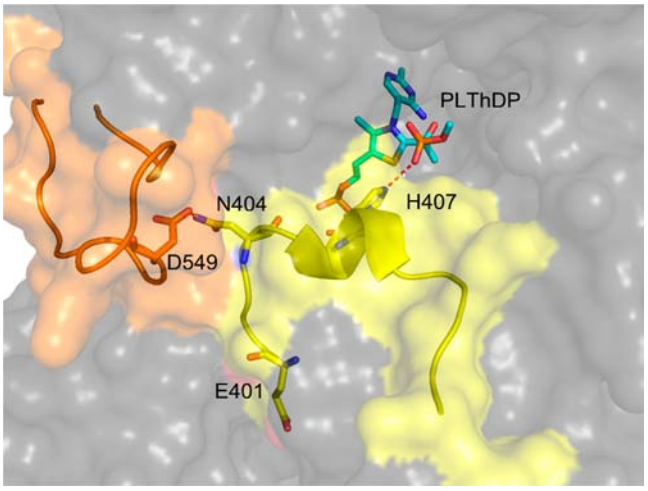

Figure 1. Dynamic loops positioned near the active site channel in E1p containing PLThDP. In the closed conformation, the ThDP C2 atom and MAP only are exposed to the solvent accessible channel. H407 from the inner loop (401–413, yellow ribbon, surface) makes H-bond contact with the intermediate analogue. D549 from the outer loop (541–557; orange ribbon, surface) makes H-bond contact with N404. Figure illustrated using PyMol v 1.4.1 with coordinates from PDB ID 2G25.

the inner loop revealed that the loops adopt two conformations in a dynamic equilibrium during the unliganded state, and the binding of a substrate analogue, methyl acetylphosphonate (MAP), shifts this equilibrium to the closed state.[8,9] ^{19}F NMR experiments revealed that the transitions occurred in the millisecond–second time scales. Stopped-flow CD studies suggested that the loop dynamics influence the covalent addition of substrate to ThDP.[9,10] On the basis of these results, we formulated "modulation of the catalytic cycle in PDHc by loop motion through coupling of dynamics and catalysis" as our working hypothesis.

To further test our hypothesis, we wanted to characterize the individual intermediates and determine their rates of transformation during the catalytic cycle of PDHc. We could then (1) assess the overall rate-limiting step(s) in the PDHc cycle, and (2) understand the effect of coupling of E1p loop dynamics to the catalytic events at the individual active sites. However, obtaining net forward rate constants for the various reactions is challenging in view of the fact that there are multiple covalent intermediates (Scheme 1A). An ingenious method to identify and quantify ThDP-bound covalent intermediates by their C6′–H ^1H NMR resonances after acid quench of enzyme reaction mixtures was invented by Tittmann and Hübner (TH).[11] ThDP-bound covalent intermediates are typically (i) stable under acid conditions, (ii) released into the supernatant, and (iii) can be simultaneously detected by their well-resolved

dx.doi.org/10.1021/ja3062375 | J. Am. Chem. Soc. 2012, 134, 18644–18655

C6′−H ^{1}H NMR resonances. As early examples of this approach, detection and kinetic characterization of covalent intermediates on the human E1p component was achieved.[12,13] To extend the capabilities of the TH method to detect and characterize ThDP-bound covalent intermediates in the complex reaction mixture of the entire multienzyme complex (4 500 000 Da), we synthesized [C2,C6′-$^{13}C_2$]ThDP. We here report transient state kinetics on PDHc and on variants created by substitutions in the two mechanistically important E1p active center loops. Using PDHc comprising E2p−E3 subcomplex together with E1p or E1p variants that was first reconstituted with specifically labeled [C2,C6′-$^{13}C_2$]ThDP, we performed 1D ^{1}H−^{13}C gradient carbon heteronuclear single quantum coherence (gCHSQC) NMR experiments. In the relevant 7.1−8.7 ppm aromatic region of the spectra, protons attached to ^{13}C only were prominent and thus enabled detection of ThDP-related resonances even in the presence of large concentrations of aromatic substrates, products, and cofactors such as NAD^+, NADH, CoA, acetyl-CoA, FAD, and $FADH_2$. Direct mass spectral detection of the rate of reductive acetylation of an E2p lipoyl domain construct in the presence of E1p and pyruvate under steady-state and single-turnover conditions provided lower limits for the rate of acetyl transfer between the ThDP of E1p and lipoamide of the E2p component.

The results suggest that formation of the first covalent predecarboxylation intermediate C2α-lactylthiamin diphosphate (LThDP in Scheme 1A) is rate limiting for the initial series of steps leading to the enamine intermediate, and in steps culminating in acetyl-CoA formation. For the first time, we could also assess the effects of complex assembly on some individual rate constants and found that assembly modestly ameliorated the rates of impaired active center dynamic loop variants, suggesting that in the complex the loop dynamics that control covalent catalysis are modulated by complex assembly.

MATERIALS AND METHODS

Materials. ThDP, NAD^+, CoA, dithiothreitol (DTT), and isopropyl β-D-1-thiogalactopyranoside (IPTG) were from USB (Cleveland, OH); 2,6-dichlorophenolindophenol (DCPIP), sodium pyruvate, and trichloroacetic acid (TCA) were from Sigma (St. Louis, MO). [C3-^{13}C]pyruvate, DCl, and D_2O were from Cambridge Isotope Laboratories (Andover, MA). All HPLC grade solvents were purchased from Sigma (St. Louis, MO). Wizard Plus Minipreps DNA Purification System was from Promega (Madison, WI). Synthesis of [C2,C6′-$^{13}C_2$]ThDP is described in detail in the Supporting Information.

Bacteria, Plasmids, Protein Overexpression, and Purification. The methods for plasmid purification, protein overexpression, and purification were described earlier.[7,9,10,14] On the basis of our early observations that the kinetic behavior of 1-lip PDHc was very similar to that of 3-lip PDHc,[15] the 1-lip E2p and its truncated versions of LD-E2p and DD-E2p were created.[14] The lipoyl domain in 1-lip E2p component is a hybrid lipoyl domain. The 85-amino acid residues starting from the N-terminus comprise residues 1−33 from the N-terminal end of the first lipoyl domain and residues 238−289 from the C-terminal end of the third lipoyl domain of the wild-type 3-lip E2 component.[16]

Enzyme Activity Measurements. Overall PDHc activity was measured by reconstitution of E1p variants with independently expressed 1-lip E2p and E3 components as described earlier.[17] The E1p component-specific activity was determined by monitoring the reduction of DCPIP at 600 nm.[18] The E1p component-specific acetaldehyde production was coupled to conversion of acetaldehyde to ethanol by yeast alcohol dehydrogenase in the presence of NADH.[19] The activity was measured in the presence of 5 mM pyruvate in standard assay buffer [20 mM KH_2PO_4 (pH 7.0), 0.5 mM ThDP, 2 mM $MgCl_2$, 0.2 mg/mL NADH, 0.08 mg/mL yeast alcohol dehydrogenase] at 30 °C. The reaction was started with addition of 0.05 mg/mL (0.5 μM) E1p, and the disappearance of NADH was monitored at 340 nm using a Varian DMS 300 spectrophotometer.

Reconstitution of Apoenzymes with [C2,C6′-$^{13}C_2$]ThDP. E1p and 1-lip PDHc apo-enzymes (free of ThDP) were prepared by dialysis of the holoenzyme twice (4 h at 4 °C) against 2 L of dialysis buffer [20 mM KH_2PO_4 (pH 7.0) 0.1 mM DTT, 0.1 mM benzamidine·HCl]. All stock solutions and dilutions were made in the reaction buffer [20 mM KH_2PO_4 (pH 7.0)]. [C2,C6′-$^{13}C_2$]ThDP stock solution (10 mM) was prepared in 20 mM KH_2PO_4 (pH 5.5).

2.5 mL of a solution of E1p or variant (0.20 mM active sites) purified in the apoenzyme form was incubated with 1 equiv of [C2,C6′-$^{13}C_2$]ThDP (0.20 mM) and Mg^{2+} (2.5 mM) for 30 min at 4 °C. Reconstitution was tested by DCPIP assay of small aliquots (10 μL). 2.5 mL of 1-lip PDHc purified in the apoenzyme form (0.20 mM active sites of E1p) was incubated with 1 equiv of [C2,C6′-$^{13}C_2$]ThDP (0.20 mM) and Mg^{2+} (2.5 mM) for 30 min at 4 °C. Reconstitution was tested by overall PDHc assay of small aliquots (10 μL).

1-lip PDHc containing E1p variants was assembled from individual components as follows: 2.5 mL of E1p variant (0.20 mM) purified in the apoenzyme form was incubated with an equal part by protein content (1:1:1 mg of E1:E2:E3) of 1-lip E2p, and E3 was added from stock. This assembled complex was incubated for 30 min at 4 °C. Next, this mixture was loaded into an Amicon Centriprep 5 mL unit and diluted with the reaction buffer. This diluted mixture was centrifuged at 2900g at 4 °C for 20 min. This washing step was repeated three more times. The final concentration of the reconstituted apo 1-lip PDHc was adjusted to 0.20 mM with reaction buffer [20 mM KH_2PO_4 (pH 7.0)] and was incubated with 1 equiv of [C2,C6′-$^{13}C_2$]ThDP (0.20 mM) and Mg^{2+} (2.5 mM) for 30 min at 4 °C. Reconstitution was tested by overall PDHc assay of 10 μL aliquots.

Rapid Chemical Quench and NMR Methods. [C2,C6′-$^{13}C_2$]-ThDP labeled enzyme was loaded into syringe A and pyruvate was loaded into syringe B in a rapid chemical quench apparatus (Kintek RQF-3 model, Kintek Corp.). A quench solution (12.5% TCA in 1 M DCl/D_2O) was loaded into syringe C. Enzyme and pyruvate solutions were mixed rapidly in a 1:1 volume ratio by a computer-controlled drive-plate and incubated for predetermined times in a reaction loop. After this incubation period, the reaction mixture was mixed rapidly with the quench solution from syringe C, and the resulting mixture was collected. For longer time scales (>10 s), the samples were assembled similarly into three different solutions. Next, equal volumes of the enzyme (200 μL) and substrate (200 μL) solutions were mixed in an Eppendorf tube, and after predetermined times the reaction was stopped by addition of quench solution (200 μL). The contents of the syringes were varied to monitor the following different reactions:

(1) For E1p with pyruvate single turnover, syringe A contained E1p (0.20 mM) reconstituted with [C2,C6′-$^{13}C_2$]ThDP (0.20 mM) in reaction buffer; syringe B contained pyruvate (20 mM) in reaction buffer.
(2) For E1p and DCPIP reductase reaction, syringe A contained E1p (0.20 mM) reconstituted with [C2,C6′-$^{13}C_2$]ThDP (0.20 mM) in reaction buffer; syringe B contained pyruvate (20 mM) and DCPIP (4 mM) in reaction buffer.
(3) For the overall PDHc oxidoreductase reaction, syringe A contained 1-lip PDHc (0.20 mM) reconstituted with [C2,C6′-$^{13}C_2$]ThDP (0.20 mM), NAD^+ (5 mM), and CoA (2 mM) in reaction buffer; syringe B contained pyruvate (20 mM).
(4) To monitor acetyl-CoA formation, syringe A contained 1-lip PDHc (0.02 mM), ThDP (2 mM), Mg^{2+} (2.5 mM), NAD^+ (5 mM), and CoA (2 mM) in reaction buffer; syringe B contained [C3-^{13}C]pyruvate (5 mM).

The quenched reaction mixture was collected and centrifuged at 15 700g for 30 min, the supernatant was separated and filtered through Gelman 0.45 μM discs, and the filtrate was analyzed by gCHSQC NMR. All NMR experiments were carried out on a Varian 600 MHz

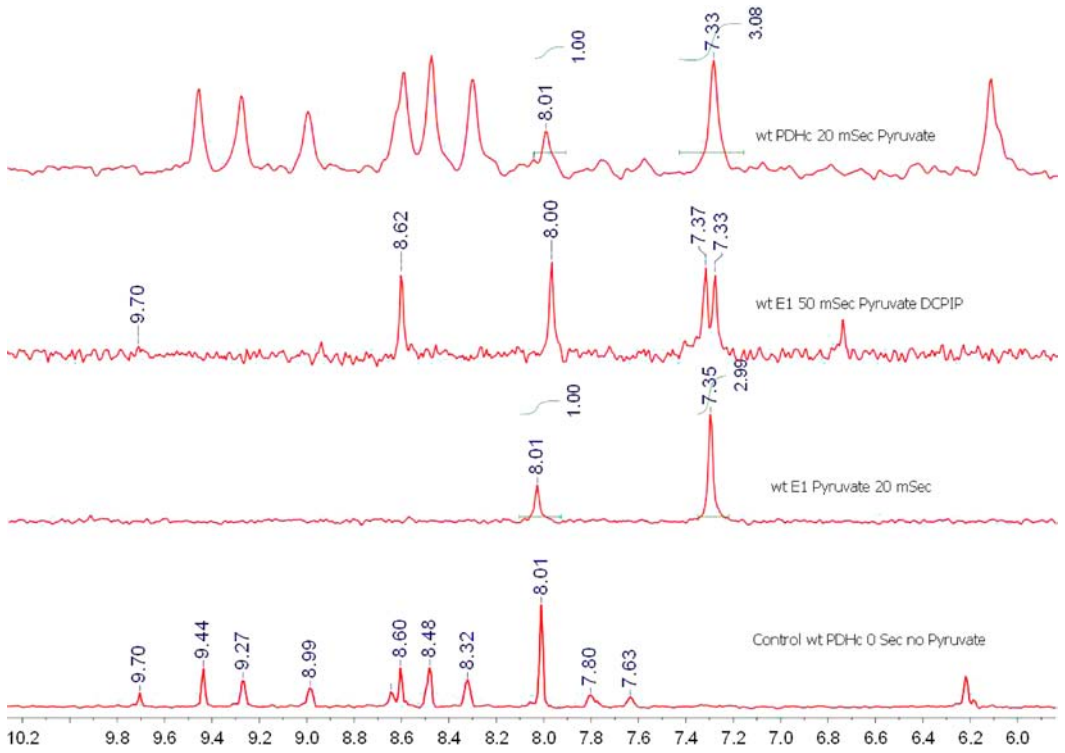

Figure 2. Distribution of ThDP-bound covalent intermediates in reactions of E1p and PDH complex. gCHSQC NMR spectra of the supernatant after acid quench of PDHc and removal of protein from the reaction. From top: (first) 20 ms quench of the reaction of PDHc; (second) 50 ms quench of the reaction of E1p with pyruvate and DCPIP; (third) 20 ms quench of the reaction of E1p with pyruvate; and (fourth) control, PDHc reaction mixture quenched before addition of pyruvate. ThDP-derived peaks are marked at 9.71 ppm (C2−H), 8.62 ppm (AcThDP), 8.01 ppm (C6′−H), 7.37 ppm (AcThDP), and 7.34 ppm (HEThDP). Other peaks are due to NAD^+, CoA, DCPIP, NADH, acetyl-CoA, or $DCPIPH_2$.

NMR instrument. Data acquisition was at 25 °C, and sample pH was ~0.75. 16 384 transients in the ^1H dimension were collected with a recycle delay time of 2 s.

The relative integrals of C6′−H signals of respective ThDP-bound covalent intermediates represent their relative ratios after correction for the amount of unbound ThDP estimated using eq 2.

$$[\mathrm{E-ThDP}] = \frac{[\mathrm{ThDP}]_0 + [\mathrm{E}]_0 + K_\mathrm{D}}{2} - \sqrt{\frac{([\mathrm{ThDP}]_0 + [\mathrm{E}]_0 + K_\mathrm{D})^2}{4} - [\mathrm{ThDP}]_0[\mathrm{E}]_0}$$

$$[\mathrm{ThDP}] = [\mathrm{ThDP}]_0 - [\mathrm{E-ThDP}] \quad (2)$$

Here, [E−ThDP] represents the concentration of E−ThDP complex; [ThDP] and $[\mathrm{ThDP}]_0$ represent concentrations of free and total ThDP; K_D is the dissociation constant.

Time course of the fraction abundance of an intermediate over the total active sites present (sum total of integrals for C6′−H signals of ThDP and all ThDP-bound covalent intermediates) was fit to single exponential eq 3 or double exponential equations of the form in eq 4 or 5.

$$f = f_1 \times (1 - e^{-k_1 t}) \quad (3)$$

$$f = f_1 \times (1 - e^{-k_1 t}) + f_2 \times (1 - e^{-k_2 t}) \quad (4)$$

$$f = f_0 + f_1 \times (e^{-k_1 t}) - f_2 \times (e^{-k_2 t}) \quad (5)$$

In experiments monitoring acetyl-CoA formation, [C3-^{13}C]pyruvate was used, and the product [C2-^{13}C]acetyl-CoA was detected using the gHSQC NMR method. The C3−H signals from pyruvate in both ketone and hydrate forms and the C2−H signal from acetyl-CoA were integrated, and the time course of fraction relative abundance of product over total acetyl groups was plotted and fit to a single-exponential eq 6.

$$f = f_0 + f_1 \times (1 - e^{-k_1 t}) \quad (6)$$

Lipoylation of the E2p Lipoyl Domain and E2p Didomain in Vitro. To ensure full lipoylation of the lipoyl domain (LD-E2p, residues 1−96 in E2p) and didomain, comprising lipoyl domain, subunit binding domain, and linkers (DD-E2p, residues 1−190 in E2p) required for reductive acetylation assay, these domains were lipoylated in vitro using *E. coli* lipoyl protein ligase.[20] The reaction mixture contained in 50 mM ammonium bicarbonate (pH 7.0): ATP (1.2 mM), $MgCl_2$ (1.2 mM), lipoic acid (0.6 mM), lipoyl protein ligase (10 μM,) and lipoyl domain (60 μM) or didomain (60 μM) for 1 h at 25 °C followed by incubation overnight at 4 °C. Lipoylation was confirmed by Fourier transform ion cyclotron resonance mass spectrometry (FT-ICR MS) using an electrospray ionization (ESI) sampling method.

Reductive Acetylation of the E2p Lipoyl Domain by E1p under Steady-State Conditions. Experimental details are presented in the legend of Supporting Information Figure S3. A FT-ICR MS-based discontinuous assay method was employed to simultaneously detect LD-E2p and acetyl-LD-E2p at various times.

Reductive Acetylation of the Lipoyl Domain in a Single-Turnover Experiment. For this experiment, the lipoyl domain (40 μM) and E1p (40 μM) or H407A variant (30 μM) in 50 mM $(NH_4)_2CO_3$ (pH 7.0) containing $MgCl_2$ (8 mM) and ThDP (0.80 mM) in syringe A was mixed with pyruvate (4 mM) in syringe B, and the reaction was stopped at times of 0.005−0.15 s by addition of 83 μL of quench solution containing 50% methanol and 2% formic acid. Samples were diluted to result in a concentration of LD-E2p of 1−2 μM in 50% methanol and 0.2% formic acid and were analyzed by ESI-FT ICR-MS. The fraction of acetylated LD-E2p at different times was determined by taking a ratio of the relative intensity of the acetylated form to the total relative intensity (sum of unacetylated and acetylated

dx.doi.org/10.1021/ja3062375 | J. Am. Chem. Soc. 2012, 134, 18644−18655

LD-E2p). Time dependence of this fraction was plotted, and the data were fitted to eq 3 using Sigma Plot 10.0.

RESULTS

Detection of ThDP-Bound Covalent Intermediates by NMR. Isotopically labeled [C2,C6′-$^{13}C_2$]ThDP enabled selective detection of ThDP-bound covalent intermediates using gCHSQC NMR experiments. In a typical ^{1}H-decoupled experiment, data were collected in the ^{1}H dimension, and only protons directly attached to ^{13}C atoms were detected. Given the 1% natural abundance of ^{13}C, [C2,C6′-$^{13}C_2$]ThDP-bound covalent intermediates could be detected and quantified even in the presence of large molar excess of aromatic cofactors over enzymes, except when ^{1}H resonances from other cofactors and intermediates overlap (Figure 2). This enabled us to extend the capabilities of the TH method to include large complexes such as the PDHc, which require additional aromatic substrates. NMR spectra from typical experiments show well-resolved resonances of [C2,C6′-$^{13}C_2$]ThDP-bound covalent intermediates in the ^{1}H dimension at the same positions as do their unlabeled counterparts in ^{1}H NMR spectra (see Supporting Information Table S1 for chemical shifts). Integration of areas under these peaks provides a quantitative estimate of their fractional abundance. The LThDP intermediate was not detected in any of our studies; presumably it did not accumulate under the various reaction conditions tested. Just as the TH method, the current method could not distinguish between the enamine and HEThDP intermediates; the former is detected as HEThDP under acid quench conditions.

Formation of LThDP Is the Rate-Limiting Step in E1p Reaction with Pyruvate. In the absence of E2p−E3 subcomplex, the E1p component converts pyruvate to acetaldehyde, and acetaldehyde release (k_{cat} = 0.12 s^{-1}) is the rate-determining step.[21] E1p reconstituted with [C2,C6′-$^{13}C_2$]-ThDP was mixed with pyruvate, and the reaction was stopped at times in the range of 0.005−30 s (see gCHSQC NMR spectra in Figure 3). Only a resonance at 7.34 ppm pertaining to the ^{13}C6′−H of HEThDP could be detected. The resonance pertaining to LThDP (7.26 ppm) could not be detected (Figure 3) and leads to the conclusion that the decarboxylation of LThDP is much faster than its formation. The transient nature of LThDP both from chemical models and during the catalysis of many pyruvate decarboxylating enzymes is discussed by Kluger and Tittmann.[22] The ^{13}C6′−H resonances for HEThDP and ThDP (at 8.01 ppm) show a time-dependent increase and decrease, respectively, indicating conversion of ThDP to HEThDP and accumulation of HEThDP in E1p active sites while approaching steady state. Integration of the signals and a correction for fraction unbound ThDP (eq 2) at each time point yields fraction relative abundance of HEThDP (Figure 3, bottom; Table 1), which fitted to a single exponential (eq 3) yields an apparent first-order rate constant of 117 ± 14 s^{-1} for formation of HEThDP. This composite rate constant includes contributions from net forward rate constants for formation of the Michaelis complex (MM, which is formed within the dead-time of the instrument), LThDP formation, and decarboxylation to enamine (Scheme 1). However, the major contribution to the rate is from the LThDP formation step (the other steps are faster), and so it can alternatively be viewed as the rate of formation of LThDP. We also emphasize that under acid quench conditions the enamine intermediate is protonated to HEThDP, its conjugate acid.

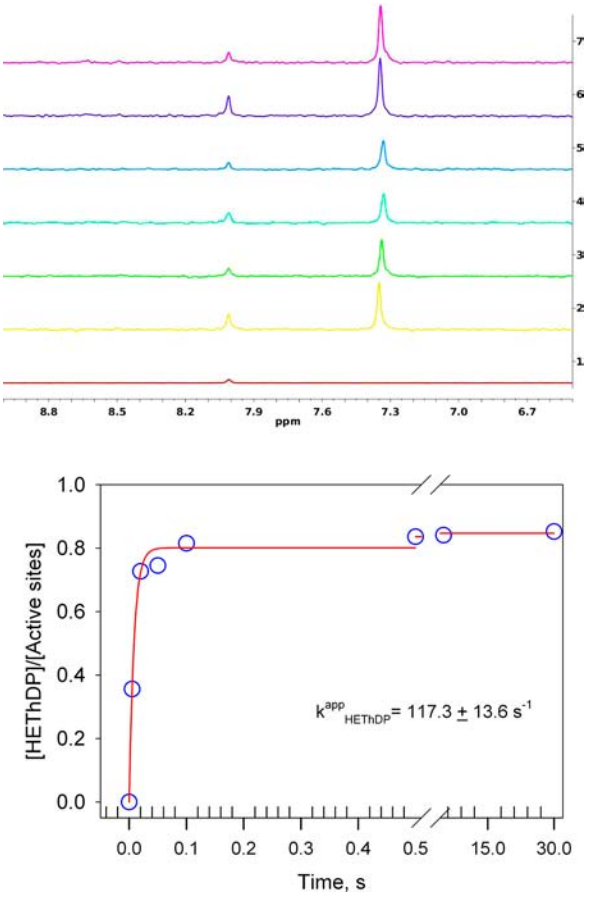

Figure 3. Distribution of ThDP-bound covalent intermediates during reaction of E1p with pyruvate. (Top) gCHSQC NMR spectra of the C6′-H resonances of ThDP-bound intermediates (6.5−9.0 ppm). Reaction of E1p (0.1 mM) with pyruvate (10 mM) was quenched in acid at the indicated times. (1) Control sample: no pyruvate, (2) 0.02 s, (3) 0.05 s, (4) 0.1 s, (5) 0.5 s, (6) 5 s, (7) 30 s. ThDP (C6′−H), δ 8.01 ppm; HEThDP (C6′−H), δ 7.34 ppm. (Bottom) Fraction HEThDP (○) calculated using ratio of C6′−H signal of HEThDP to total C6′−H signals from HEThDP and ThDP determined at times 0, 0.005, 0.02, 0.05, 0.1, 0.5, 5, and 30 s during E1p reaction with pyruvate. The data points were fit using eq 8, and the line is the regression fit trace.

Chemical Oxidation of the Enzyme-Bound Enamine Affords Transient Detection of AcThDP on E1p. The central enamine intermediate reductively acetylates the lipoamide group on E2p, a reaction that can be viewed as (1) a 2-electron oxidation to 2-acetyl-ThDP and concomitant reduction to dihyrolipoyl-E2p, followed by (2) transfer of the resultant acetyl group to the dihydrolipoyl-E2p with the dithiolane ring of lipoamide participating in both steps. In related oxidative decarboxylases such as pyruvate oxidase and pyruvate ferredoxin oxidoreductase, the enamine is oxidized by enzyme-bound cofactors such as FAD or FeS clusters, respectively, and the resultant acetyl moieties are transferred to phosphate or CoA acceptor groups, respectively. This allows accumulation of 2-acetylthiamin diphosphate (AcThDP) in the latter enzymes when the acceptors are absent.[23−25] However, during the overall PDHc pathway, because the lipoamide serves both functions and AcThDP does not appear to accumulate at significant levels as shown by Frey et al.,[26] this hinders pre-steady-state studies aimed at determining the rates of oxidation. Alternatively, an artificial electron acceptor can be used to study

dx.doi.org/10.1021/ja3062375 | J. Am. Chem. Soc. 2012, 134, 18644−18655

Table 1. Comparison of Pre-Steady-State Rate Constants for E1p and Variants under Various Conditions

		k_{HEThDP} (s^{-1})			
variant	k_{cat},[a] s^{-1}	pyruvate only	pyruvate + DCPIP	PDHc reaction[b]	k_r (s^{-1}) reductive acetylation[c]
E1p	95 ± 12	117 ± 14	73.2 ± 8.8	116 ± 25	51.7 ± 5.4
D549A	0.7 ± 0.1	12.9 ± 1.0		12.1 ± 0.5	
H407A	0.08 ± 0.01	1.16 ± 0.05	0.06 ± 0.01	2.5 ± 0.19	0.02 ± 0.001
E401K	0.83 ± 0.05	0.13 ± 0.02	0.016 ± 0.003	0.59 ± 0.05	
Y177A	3.31 ± 0.3	25.9 ± 1.2			

[a]The k_{cat} values were determined from the overall PDHc activity assay on reconstitution with E2−E3 subcomplex. [b]E1p-specific reaction with DCPIP assay on reconstitution with E2−E3 subcomplex. [c]For reaction of reductive acetylation of LD-E2p with E1p or variant and pyruvate using ESI-FT-MS.

the oxidation step of E1p with pyruvate, and DCPIP as a two-electron acceptor is commonly used to assay ThDP-dependent oxidative decarboxylases. DCPIP (monitored at λ_{max} = 600 nm, Scheme 1B) oxidizes the central enamine intermediate producing the reduced form $DCPIPH_2$. While the k_{cat} of 0.65 ± 0.16 s^{-1} determined by this assay is 100-fold lower than the overall k_{cat} of 95 ± 12 s^{-1} for PDHc, DCPIP serves as a quick and efficient assay to study oxidation of the enzyme-bound enamine for E1p variants, confirming that decarboxylation has taken place.

In pre-steady-state experiments, acid quench of reaction mixtures of E1p reconstituted with [C2,C6′-$^{13}C_2$]ThDP with pyruvate and DCPIP during 0.005−30 s, the NMR spectra revealed resonances at 7.34 ppm for ^{13}C6′−H of HEThDP, and at 7.36, 7.37, and 8.62 ppm for the ^{13}C6′−H of AcThDP (acetyl, hydrate, and internal carbinolamine forms), but none for LThDP (Figure 4). The resonance for HEThDP displays a time-dependent increase reaching a steady state during early times (0−0.5 s). The resonances for AcThDP show a time-dependent rapid increase during short time scales (0.0−0.5 s) and a decrease at longer time scales (0.5−30 s) corresponding to the total consumption of DCPIP, and subsequent slow hydrolysis of AcThDP to acetate and ThDP. Data treatment, as described above, yielded an apparent first-order rate constant of 57 ± 6 s^{-1} for AcThDP formation and 73.2 ± 8.8 s^{-1} for enamine formation (Figure 4, bottom inset; Table 1). It is assumed that the total amount of enamine during any time point is the sum total of AcThDP and HEThDP). The fractional abundance of AcThDP was also fit to a biexponential process (eq 5) yielding an apparent rate constant of 52 ± 7.5 s^{-1} for AcThDP formation, and a first-order rate constant of 0.23 ± 0.05 s^{-1} for its hydrolysis (Figure 4, bottom; see also Table 2 in the Discussion).

The kinetic data show that the enamine is rapidly oxidized on E1p in the presence of DCPIP.[27]

The hydrolysis of AcThDP appears to be the slow step (k'_5 = 0.23 ± 0.05 s^{-1}; see Scheme 2A in the Discussion) explaining the discrepancy between the steady-state k_{cat} values derived from the DCPIP-based assay (0.65 ± 0.16 s^{-1}) and PDHc activity-based assay (95 ± 12 s^{-1}). While the enamine is oxidized by DCPIP at a rate comparable to its formation (see above), the AcThDP intermediate thus generated is hydrolyzed at a very slow rate, similar to the nonenzymatic hydrolysis rate of synthetic 2-acetylThDP at pH values of 7−7.5.[28] Even when bound to enzyme, the rate of AcThDP hydrolysis is unaffected, hence the low k_{cat}. Nevertheless, the DCPIP-based artificial oxidation reaction is a relevant model for studying the oxidation of the enamine on ThDP dependent oxidative decarboxylases at the individual active site level using pre-steady-state kinetics (Scheme 1B). While the mechanism of this artificial oxidation step is unclear (location of DCPIP on the enzyme, electron transfer pathway, etc.), it is clear that AcThDP is the intermediate in this reaction.

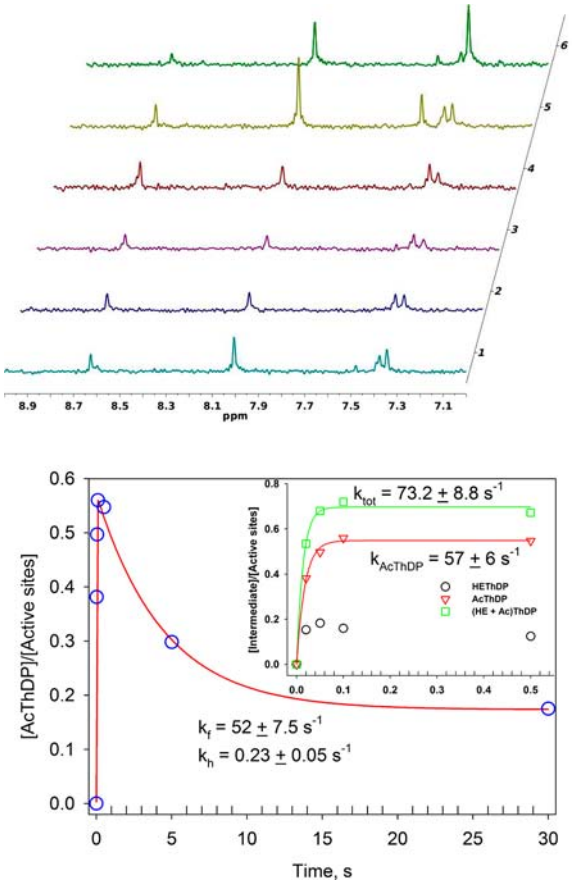

Figure 4. Distribution of ThDP-bound covalent intermediates during the reaction of E1p with pyruvate and DCPIP. (Top) gCHSQC NMR spectra of the C6′−H resonances of ThDP-bound intermediates (6.5−9.0 ppm). Reaction of E1p (0.1 mM) with pyruvate (10 mM) and DCPIP (2 mM) was quenched in acid at the indicated times. (1) 0.02 s, (2) 0.05 s, (3) 0.1 s, (4) 0.5 s, (5) 5 s, (6) 30 s. ThDP (C6′−H), δ 8.01 ppm; HEThDP (C6′−H), δ 7.34 ppm; 2-acetylThDP (C6′−H), δ 8.62 ppm (carbinolamine), 7.38 and 7.37 ppm (hydrate and keto forms). (Bottom) Time course of AcThDP: Steady state is reached within 0.5 s; next, consumption of DCPIP leads to depletion of AcThDP and formation of HEThDP. The red trace is the regression fit line to eq 5. (Inset) Fraction intermediate (AcThDP (red), HEThDP (black)) calculated using ratio of C6′−H signals of intermediate to total C6′−H signals from AcThDP, HEThDP, and ThDP determined during the first 0.5 s.

dx.doi.org/10.1021/ja3062375 | J. Am. Chem. Soc. 2012, 134, 18644−18655

ThDP-Bound Covalent Intermediates on E1p during the Full Catalytic Cycle of PDHc. Having confirmed that the major ThDP-bound covalent intermediates could be detected in a time-resolved manner using our method, PDHc was reconstituted in the presence of all substrates to determine: (a) the fate of the covalent intermediates during the catalytic cycle and (b) if complex assembly has any effect on catalysis in the E1p active sites. PDHc reconstituted with [C2,C6′-$^{13}C_2$]ThDP was mixed with pyruvate, CoA, and NAD^+, and the reaction was stopped at 0.005−30 s (Figure 5). As with E1p alone, only

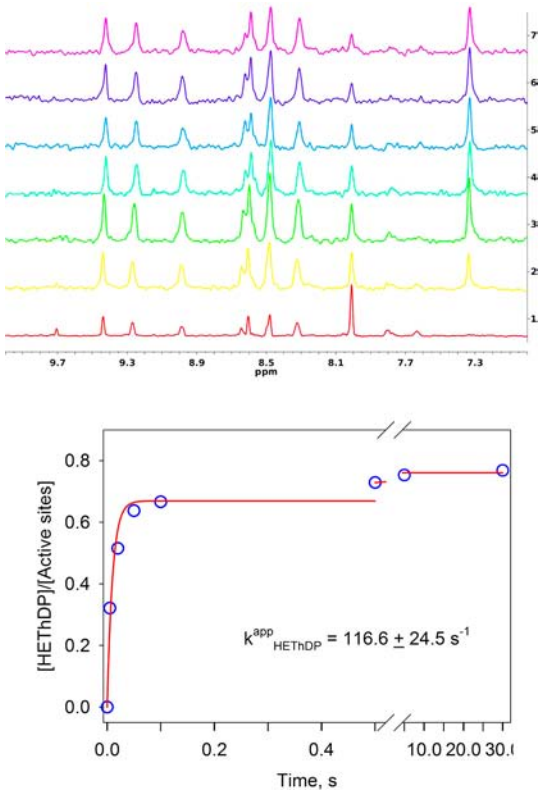

Figure 5. Distribution of ThDP-bound covalent intermediates during PDHc reaction. (Top) gCHSQC NMR spectra of the C6′−H resonances of ThDP-bound intermediates (6.5−9.0 ppm). Reaction of E1p (0.1 mM) with pyruvate (10 mM), NAD^+ (2.5 mM), and CoA (1 mM) was quenched in acid at the indicated times. (1) Control sample: PDHc and cofactors without pyruvate, (2) 0.02 s, (3) 0.05 s, (4) 0.1 s, (5) 0.5 s, (6) 5 s, (7) 30 s. ThDP (C6′−H), δ 8.01 ppm; HEThDP (C6′−H), δ 7.34 ppm. Other peaks due to NAD^+, CoA substrates, and NADH and acetyl-CoA products. (Bottom) Fraction HEThDP (○) calculated using ratio of C6′−H signal of HEThDP to total C6′−H signals from HEThDP and ThDP determined at various times (0, 0.005, 0.02, 0.05, 0.1, 0.5, 5, 30 s) during the PDHc overall reaction. The trace is the regression fit line to eq 3.

HEThDP could be detected at all times; that is, LThDP and AcThDP do not accumulate to detectable levels. Two studies on the transient nature of the AcThDP during PDHc catalysis showed that (i) it was chemically competent and could be transferred to the dihydrolipoate when generated on the enzyme using 3-fluoropyruvate, and (ii) using [C3-^{14}C]-pyruvate, 0.5% of PDHc active sites were found to contain AcThDP during the overall PDHc reaction, while up to 12% of active-sites were found to contain AcThDP in an artificial enamine oxidation reaction using ferricyanide.[28,29] These results are similar to the current findings using the NMR method. While AcThDP could be detected during the artificial oxidation reaction, it presumably does not accumulate to detectable levels according to NMR during the overall PDHc reaction. This is consistent with the following scenarios: (i) the rate of acetyl transfer from E1p to dihydrolipoylE2p is faster than the rate of oxidation of the enamine to AcThDP in a stepwise mechanism, or (ii) a concerted reductive acetylation mechanism proceeding by a tetrahedral intermediate transiently cross-linking the E1p and lipoylE2p, without a distinct AcThDP accumulating, as modeled by Pan and Jordan.[30]

The resonances for HEThDP and ThDP display a time-dependent increase and decrease, respectively, indicating a conversion of ThDP to HEThDP. Analysis (eq 3) yields a fraction of relative abundance of HEThDP leading to an apparent first-order rate constant of 117 ± 25 s^{-1} for the formation of HEThDP (Figure 5, bottom; see also Tables 1 and 2), as compared to the overall k_{cat} of 95 ± 12 s^{-1} determined from V_{max} (57 ± 7 activity units per E1 active center) for NADH production for 1-lip PDHc.

Conversion of Pyruvate to Acetyl-CoA. We also tested the kinetic competence of the intermediates by directly monitoring the conversion of [C3-^{13}C]pyruvate to [C2-^{13}C]-acetylCoA by PDHc using gCHSQC NMR (Supporting Information Figure S1). Quantification using integration of ^{13}C bound ^{1}H signals yielded an initial velocity of 1219 ± 66 μM/s for acetyl-CoA production under the reaction conditions (10 μM E1p active centers in the reaction loop). Assuming full saturation of all components, this initial velocity corresponds to a k_{cat} of 122 ± 6.6 s^{-1} per E1p active centers (Supporting Information Figure S1, bottom), a number remarkably similar in magnitude to the other rate constants on the pathway determined in this work (Table 1).

Reductive Acetylation of LD-E2p Is Not the Rate-Limiting Step in the Overall PDHc Reaction. Reductive acetylation of the lipoyl moiety covalently bound to the lipoyl domain of E2p is the final step involving ThDP-bound covalent intermediates. The reaction of enamine derived from C2α-methoxybenzyl-3,4,5-trimethylthiazolium salt with *S*-methyllipoic acid methyl ester, a mimic of the S-protonated form, was shown to be a chemically competent model for this step.[30] The free lipoic acid itself is a poor substrate both in chemical models[31] and for E1p-bound enamine.[32] Also, E1p has been shown to successfully reductively acetylate the independently expressed LD-E2p,[6,7] providing the most appropriate model reaction to study the rate of the final step in E1p catalysis while conserving both the chemistry and the intercomponent communication due to its specific recognition of E1p.[33−35] Therefore, a method was developed to detect LD-E2p and acetyl-LD-E2p simultaneously in the quenched reaction mixtures using ESI-FT-ICR MS (Supporting Information Figure S2). Fortuitously, the acetyl-LD-E2p and indeed the acetyl-DD-E2p are stable under the reaction and MS conditions.

Reductive Acetylation of LD-E2p under Steady-State Conditions. First, the reductive acetylation by E1p (5 nM) was monitored at varying concentrations of LD-E2p (1.5−20 μM) in the presence of 2 mM pyruvate. Under these conditions, the LD-E2p is a substrate for E1p, and during multiple turnovers the acetylated LD-E2p accumulates as the product of the reaction (Supporting Information Figure S3 and Figure 6). A plot of the initial slope/min calculated from the progress curve of a time-dependent accumulation of acetylated LD-E2p versus concentrations of LD-E2p resulted in a

dx.doi.org/10.1021/ja3062375 | J. Am. Chem. Soc. 2012, 134, 18644−18655

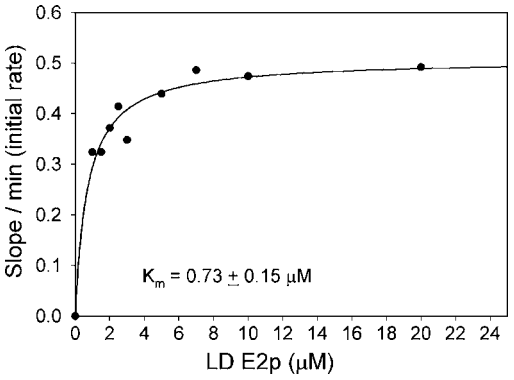

Figure 6. Michaelis–Menten plot for steady-state reductive acetylation of LD-E2p by E1p and pyruvate. For experimental details, see legend of Figure S3. Data were fitted to a Michaelis–Menten equation ($v_o = v_o^{max}[\text{LD-E2p}]/(K_m + [\text{LD-E2p}])$, and the trace is the regression fit line.

hyperbolic curve yielding a K_M of 0.73 ± 0.15 μM for LD-E2p (Figure 6), a much lower value than the 26 μM reported earlier.[32]

Pre-Steady-State Kinetics of Reductive Acetylation of LD-E2p by E1p. The K_M for LD-E2p from above suggested conditions for a single turnover kinetic experiment, a better model of the reductive acetylation as it occurs during PDHc catalysis. At high concentrations of E1p (40 μM active sites) and LD-E2p (40 μM), formation of the E1p–LD-E2p complex is ensured to be spontaneous, and chemical steps become rate limiting in a pseudo first-order process. Also, in contrast to steady-state conditions described above, single turnover conditions ensure that product release steps do not impede rates. Samples collected in the time range of 0.005–0.15 s were analyzed using ESI–MS, and a rate constant of 52 ± 5 s^{-1} for reductive acetylation of LD-E2p by E1p was calculated (Figure 7, top). In a similar experiment, a value of 50 ± 5 s^{-1} confirmed reproducibility of the data (not shown). This pseudo first-order rate constant is composed of the rates of conversion of pyruvate to the enamine and the reductive acetylation of the lipoyl domain by the enamine (Scheme 1A). Because the rate constant for reductive acetylation of LD-E2p (52 s^{-1}) was lower than that of acetyl-CoA formation (k_{cat} = 122 s^{-1}), a similar experiment was also conducted with an E2p didomain comprising the lipoyl domain, the subunit-binding domain, and linker regions (DD-E2p), presenting a better mimic of E2p by providing a binding domain for E1p. Rate constants of 134 and 96 s^{-1} (Figure 7, bottom) were obtained in two independent experiments, also clearly indicating that reductive acetylation of the lipoyl domain is not a rate-limiting step in the overall PDHc reaction.

In contrast, the H407A substitution in E1p drastically reduces the rate of reductive acetylation of LD-E2p and DD-E2p, lowering the rate constants to 0.02 ± 0.001 s^{-1} (LD-E2p) and 0.04 ± 0.01 s^{-1} (DD-E2p) (Table 1), indicating that the residue His 407 participates in communication between E1p and E2p, as was suggested earlier.[6,7] Moreover, for this variant, reductive acetylation becomes rate determining, as the preceding steps up to formation of HEThDP (2.5 s^{-1}) are 50-fold faster in the reaction reconstituting H407A E1p to PDHc (Table 1 and Supporting Information Figure S5).

Substitutions at the Mobile Active-Center Loops Impair the First C–C Bond Formation Step. Next, to test the role of active center dynamic loops on individual catalytic

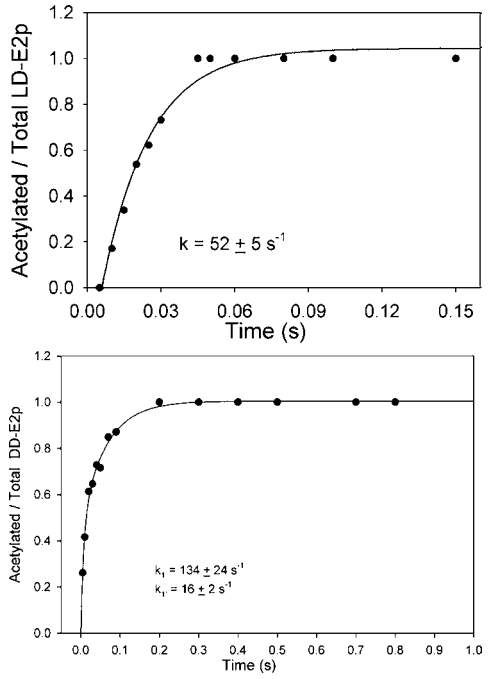

Figure 7. Time-dependence of fraction acetylated LD-E2p and DD-E2p during single turnover reaction. Top: The LD-E2p (40 μM) and E1p (concentration of active centers/subunit = 40 μM) in syringe A was mixed at 25 °C with pyruvate (4 mM) in syringe B (see details under Materials and Methods). Reaction was stopped at times 0.005–0.15 s by addition of quench solution, and samples were analyzed by FT ICR- MS. The intensity of the MS signal for acetylated and unacetylated LD-E2p was detected. The relative intensity of acetylated LD-E2p versus total intensity (sum of acetylated and unacetylated LD-E2p) was plotted versus time. Data were fitted to a single exponential (eq 3). Bottom: The E1p (concentration of active centers/subunit = 30 μM) and DD-E2p (30 μM) in 50 mM ammonium bicarbonate (pH 7.0) containing 0.4 mM ThDP and 2.0 mM $MgCl_2$ in syringe A were mixed at 25 °C with pyruvate (4 mM) in 50 mM ammonium bicarbonate (pH 7.0) in syringe B. Reaction was stopped at times 0.005–1.0 s by addition of quench solution, and samples were analyzed by FT ICR-MS. Data were fitted to a double exponential (eq 4).

steps, we selected E401K (inner loop hinge residue substitution), H407A (inner loop His interacting with PLThDP), and D549A (outer loop Asp interacting with inner loop Arg404) for pre-steady-state kinetic studies (see Figure 1).

In an experiment similar to that carried out with E1p, loop variants (E401K, H407A, D549A, or Y177A E1p) were reconstituted with [C2,C6′-$^{13}C_2$]ThDP and mixed with pyruvate, and the reactions were stopped at 0–300 s. Only the resonance at 7.34 ppm pertaining to the ^{13}C6′–H of HEThDP could be detected for all variants at all time points, again indicating no LThDP accumulation in any of the loop variants tested. Data treatment yielded apparent first-order rate constants for formation of HEThDP (Supporting Information Figures S4–S6, and Table 1). The rates decrease in the following order: E1p > Y177A > D549A > H407A > E401K, with increasing disruption of loop dynamics expected from these substitutions. The Y177A E1p, a substitution in a nonmobile active-site loop, was used as a control for nonspecific effects of disruptions to the active site and showed only a 4-fold reduction as compared to E1p (Supporting Information Figure S7, and Table 1), whereas substitutions in the dynamic loops elicited reductions of 10–900-fold. These

dx.doi.org/10.1021/ja3062375 | J. Am. Chem. Soc. 2012, 134, 18644–18655

apparent rate constants, which represent the rates of formation of LThDP, indicate that the substitutions dramatically impair the first C−C bond formation step. We also note that we cannot determine the effect of these substitutions on the rate of LThDP decarboxylation relative to E1p.

The 100-fold rate reduction observed in the H407A E1p variant, where the H-bond connecting the inner loop to the predecarboxylation intermediate is abolished, suggests a significant role for this interaction in the predecarboxylation steps. The drastic reduction of a 900-fold in the case of E401K E1p (charge reversal substitution at a hinge residue), in conjunction with the disordered loops seen in the structure of E401K E1p in presence of PLThDP,[7] suggests that active-site sequestration, to avoid carboligase-type side reactions, is also essential for formation of the first C−C bond.

Enamine Oxidation by DCPIP in Inner Loop E1p Variants. When using DCPIP to convert the enamine to 2-acetylThDP, unlike with E1p, only HEThDP could be detected in both E401K E1p and H407A E1p. The rates of HEThDP formation (0.13 s^{-1} for E401K E1p, and 1.16 s^{-1} for H407A E1p) with pyruvate as the only reactant are similar to the rate of hydrolysis of AcThDP (0.23 s^{-1}) accounting for our inability to observe significant buildup of this intermediate (Supporting Information Figures S4−S6; see also Tables 1 and 2). Also, the apparent rates of HEThDP accumulation in these experiments (0.016 s^{-1} for E401K E1p) and (0.06 s^{-1} for H407A E1p) are much lower than the corresponding rates in the absence of DCPIP as presented above.

Assembly to PDHc improves reaction rates of E1p mobile active-center loop variants suffering from drastically impaired rates.

Next, the effect of reconstitution of the mobile loop variants (E401K E1p, H407A E1p, and D549A E1p) with E2p−E3 subcomplex on catalysis was determined in the presence of pyruvate, NAD^+, and CoA. Similarly to all earlier experiments, only HEThDP could be detected during the various time scales, without apparent accumulation of LThDP. The apparent rates of formation of HEThDP for reconstituted PDHc reactions are summarized in Table 1 (also see Supporting Information Figures S4−S6). Again, these apparent rate constants, which represent the rates of formation of LThDP, decrease in the order E1p > D549A > H407A > E401K, in direct relation to increasing disruption of loop dynamics expected from these substitutions.

Comparison of the rates of E1-specific reactivity (reaction with pyruvate only) of parental and variant E1p's provided additional insights. There is an approximately 5-fold improvement in the rate of HEThDP formation for E401K E1p, 2-fold improvement for H407A E1p, and no change for D549A E1p and for the E1p on assembly to complex. These results suggest that assembly of complex has a modest yet clearly discernible effect on catalysis by the E1p component. Presumably, the interaction with lipoyl domains of E2p orders the inner loop over the E1p active site leading to a modest recovery in active-site sequestration. This PDHc assembly induced recovery is maximal for the highly disrupted inner loop variants, and there is no change for the outer loop variant or the PDHc.

DISCUSSION

Pioneering efforts in the syntheses and characterization of central ThDP-bound covalent intermediates opened up avenues for the application of NMR methods to thiamin enzymology leading to the development of the current state-of-the-art.[22] During the course of this study, synthesis of [C2,C6′-$^{13}C_2$]ThDP provided the first observation by NMR of the fate of ThDP-bound covalent intermediates during catalysis by the entire PDHc from *E. coli*. In studies with model C2α-lactylthiazolium salts, Zhang et al. showed the rate of decarboxylation increased with decreasing solvent polarity from water to tetrahydrofuran, and in tetrahydrofuran the first-order rate constant exceeds 50 s^{-1}.[36] Presumably, the E1p active site provides such a hydrophobic environment. In studies using HEThDP as a substrate for E1p, Zhang et al. estimated up to 10^7-fold rate acceleration for ionization of the C2α−H bond of HEThDP bound to E1p. This rate acceleration corresponds to 10 kcal/mol stabilization of the enamine intermediate on the enzyme,[27] and thus channels this electron-rich intermediate (the enamine) toward oxidation by the lipoyl moiety covalently attached to E2p. The free lipoic acid is a poor acceptor as compared to an analogue mimicking its protonated form in chemical models (10^8-fold rate enhancement)[30] and LD-E2p in enzymic models (k_{cat}/K_M enhancement of >10^4-fold).[32] These studies provided fundamental groundwork for our understanding of the results here presented: (a) LThDP decarboxylation could be fast with low barriers in general, unless some elements of the protein environment slow it down; (b) in E1p, the enamine is highly stabilized, and its concentration almost certainly corresponds to that of the HEThDP detected as a result of the acid quench; and (c) the catalytic contributions for reductive acetylation originate from E1p (activation of lipoic acid) and LD-E2p.

Determination of Net Forward Rate Constants. A kinetic model for catalysis in PDHc was constructed according to Cleland's net rate constants method,[37] by substituting net rate constants denoted with prime for individual forward and reverse rate constants. The net rate constants denote the flux through each step, and in case of irreversible steps, the net rate constants would be identical to the true forward rate constants (Scheme 2). For a series of reactions, the reciprocal of the net rate constant for any individual step is its transit time. This transit time model can be applied to determine each individual net rate constant as a summation of transit times of the previous steps.[11,38]

$$\frac{1}{k_{\mathrm{HEThDP}}} = \frac{1}{k'_1} + \frac{1}{k'_2} + \frac{1}{k'_3} \quad \text{and}$$

$$k_1' = \frac{k_1 \times [\mathrm{pyruvate}] \times k_2'}{k_{-1} + k_2'} = \frac{[\mathrm{pyruvate}]}{K_M} \times k_2' \qquad (7)$$

$$\frac{1}{k_{\mathrm{AcThDP}}} = \frac{1}{k_{\mathrm{HEThDP}}} + \frac{1}{k'_D} + \frac{1}{k'_4} \quad \text{where}$$

$$k'_D = \frac{k_{on} \times [\mathrm{DCPIP}] \times k_4'}{k_{off} + k_4'} = \frac{[\mathrm{DCPIP}]}{K_M^{\mathrm{DCPIP}}} \times k_4' \qquad (8)$$

$$\frac{1}{k_{\text{reductive acetylation}}} = \frac{1}{k_{\mathrm{HEThDP}}} + \frac{1}{k'_D} + \frac{1}{k'_4} \quad \text{where}$$

$$k'_D = \frac{k_{on} \times [\mathrm{LD}] \times k_4'}{k_{off} + k_4'} = \frac{[\mathrm{LD}]}{K_M^{\mathrm{LD}}} \times k_4' \qquad (9)$$

From eq 7, k_2', the net rate constant for formation of LThDP, approximates to the experimentally observed rate k_{HEThDP} for the following reasons: (i) under pyruvate saturating conditions, the Michaelis complex accumulates within 2.5 ms;[9,10] and (ii) decarboxylation is not rate limiting in any of the

dx.doi.org/10.1021/ja3062375 | J. Am. Chem. Soc. 2012, 134, 18644−18655

Scheme 2. Transit Time Kinetic Model of E1p Reaction with (A) DCPIP and (B) LD-E2p under Single Turnover Conditions Modeling PDHc

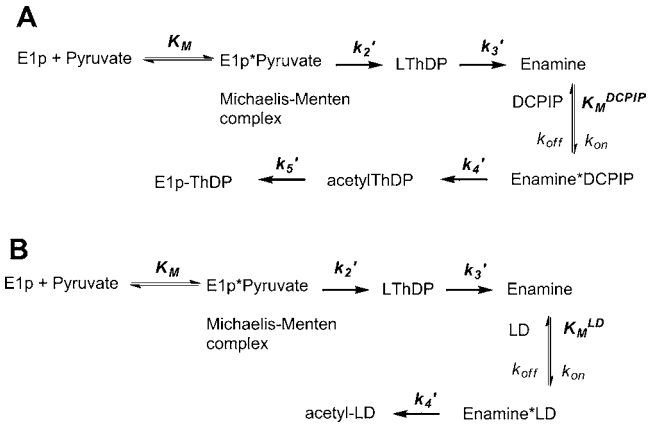

experiments with E1p or variants. The net forward rate constants, summarized in Table 2, suggest that the enamine is similarly susceptible to oxidation by DCPIP, LD-E2p, or DD-E2p. The net rate constants for reductive acetylation from this study provide a lower limit for the physiological reaction, because the attachment of the LD or DD-E2p to the core domain of E2p by the flexible linker could provide added rate enhancement by providing stringent diffusion limitations.[39] This is evident upon comparison with the overall k_{cat} (122 s^{-1}) for acetyl-CoA production by the PDHc. While reductive acetylation was believed to be the rate-limiting step in PDHc catalysis,[40] the current study provides similar net rate constants for several steps, which are within range of the overall k_{cat}, suggesting equalized barriers[41,42] for the interconversion of these intermediates by evolutionary optimization for substrate channeling.[43,44]

The Effects of Assembly on Inner and Outer Loop Variants. Thermodynamic analysis of substrate analogue MAP binding to E1p produced nonlinear van't Hoff plots (ΔC_p = −246 cal mol^{-1} K^{-1}), suggesting a coupling of a conformational change with ligand binding, and the corresponding conformational states were observed in the X-ray structure and in solution studies using NMR and EPR spectroscopy.[5,8,9] In contrast, for the H407A E1p and E401K E1p variants with rigid body binding behavior (ΔC_p = 0 cal mol^{-1} K^{-1}), the closed conformation of the loops could not be observed in the crystal structure. Our current study with substrate reveals the roles of loop dynamics during the catalytic cycle by identifying the particular catalytic step(s) and their contribution to rate enhancements during these steps. Our results suggest that, similar to PDHc, formation of the first covalent predecarboxylation intermediate LThDP is the rate-determining step for the active-site loop variants. The rate of LThDP formation tended to decrease drastically with increasingly disruptive substitutions (Tables 1 and 2). Taken together with earlier structural and thermodynamic studies, this implies that the loop dynamics and the ensuing conformational changes upon substrate binding to E1p contribute toward catalysis and LThDP formation. These results also point to a sequential mechanism for loop closure, whereby the inner loop has to close first providing a new surface for interactions and closing of the outer loop. In such a mechanism, affecting the inner loop would have strong detrimental effects on catalysis, while the effect due to disruptions of the outer loop will be of lesser importance to LThDP formation.

The effect of complex assembly in the presence of the E2p and E3 components, which can be interpreted as recovery of E1p active-site sequestration, also follows a general trend. The recovery seen is in the order E401K E1p (5-fold) > H407A E1p (2-fold) > D549A E1p = E1p (no change) from minimal to maximal recovery. Complex assembly helps maximally disrupted variants, while it has minimal effect on the outer loop variant and E1p. The overall k_{cat} and rate of reductive acetylation of the lipoyl domains are at least 10-fold lower than the rate of HEThDP formation in the loop variants (Tables 1 and 2), suggesting that in contrast to the PDHc, reductive acetylation is rate-determining in the case of the inner and outer loop variants. The active-site loops are disordered in the crystal structures of both E401K E1p and H407A E1p in the presence of PLThDP, whereas they are ordered in the E1p (see yellow surface in Figure 1), suggesting that in PDHc, the preformed surface is near optimal for interactions with the lipoyl domain; hence assembly elicits no further changes. However, in the loop variants, such a surface has to be induced upon binding of E2p to enable the observed reductive acetylation of lipoamide. Presumably, the effect of loop dynamics on catalysis has been optimized by evolution for the E1p.

The dynamic loop regions described in this study are highly conserved in other homodimeric α_2 and heterotetrameric $\alpha_2\beta_2$ E1 components of 2-ketoacid dehydrogenases, as observed in X-ray structures.[45−50] The loops that undergo dynamic equilibrium over the active sites in ThDP-dependent enzymes carry out similar functions with different triggers. For example, in human $\alpha_2\beta_2$ E1 branched chain ketoacid dehydrogenase and

Table 2. Net Forward Rate Constants for Individual Steps in Oxidative Decarboxylation Reactions of E1p

reaction	k_1', s^{-1}[a]	k_2', s^{-1}	k_3', s^{-1}[b]	k_4', s^{-1}	k_5', s^{-1} (DCPIP)
PDH complex	>600[a]	117 ± 25	fast	93.6	
E1p DCPIP	>600[a]	117 ± 25	fast	111.2	0.23 ± 0.05
E401K E1p DCPIP	>600[a]	0.13 ± 0.02	fast	0.05	0.23 ± 0.05[c]
H407A E1p DCPIP	>600[a]	1.16 ± 0.05	fast	0.13	0.23 ± 0.05[c]
H407A E1p PDHc	>600[a]	2.5 ± 0.2	fast	0.02	
chemical models[d]	3×10^{-3}	NA	50	6.6×10^4 (M^{-1} s^{-1})	0.23

[a]The Michaelis−Menten (MM) complex accumulates within 2.5 ms in E1p and loop variants.[9] [b]Because LThDP does not accumulate, we can only infer $k_3' \gg k_2'$, and consequently the effect of loop substitutions on k_3' could not be determined. k_4' is the composite net rate constant involving binding of DCPIP or lipoyl domain to E1p and reaction with enamine. k_5' is the forward rate constant for hydrolysis of 2-acetylThDP in DCPIP reaction. For PDHc and H407A PDHc, because AcThDP could not be detected, k_5' is not determined, and k_4' includes the rate for oxidation of the enamine and transfer of the acetyl group to the lipoyl domain. [c]Assuming k_5' is similar to the uncatalyzed rate. [d]The thiamin C2−H deprotonation is rate-determining in k_1'.[55]The rate constants for the chemical models are from refs 32, 28, and 29. NA is not available in the literature.

dx.doi.org/10.1021/ja3062375 | J. Am. Chem. Soc. 2012, 134, 18644−18655

human $\alpha_2\beta_2$ E1p, phosphorylation of an active site loop destabilizes the closed/ordered loop conformation,[51−53] whereas in other examples, the stabilization of closed conformation is induced by ThDP binding.[47,50,54]

In the present study, the closed conformation of the active center loops is only apparent on formation of the predecarboxylation LThDP intermediate, while the loop variants indicate potential effects of complex assembly on loop closing.

CONCLUSION

Using de novo synthesized ^{13}C-labeled thiamin and FT-MS, we have developed new approaches capable of determining the pre-steady-state rate constants for conversion of the 2-oxoacid starting material to all intermediates, also including intercomponent communication between the E1p and E2p, and formation of acetyl-CoA on E2p in the entire multimegadalton pyruvate dehydrogenase complex.

For the first time, these approaches enabled us to deduce the effect of complex assembly on microscopic rate constants. (a) The results all point to the notion that formation of the first covalent bond between substrate and the C2 atom of ThDP (formation of LThDP) is rate limiting overall, and all of the subsequent rate constants measured are very similar within experimental error. This is consistent with rather similar barriers having evolved for the various chemical conversions on the enzyme. (b) Assembly to PDHc had no effect on the rate constants on E1p, but assembly did improve the rate constants for the least active inner loop variants.

Our earlier results pointing to a relationship between the rate of formation of LThDP and mobility of dynamic active center loops make these results even more intriguing. Combining the information from this study and our previous one on loop mobility on E1p leads to the important conclusion that loop movement on the E1p component controls the rate-limiting step in the entire multienzyme complex. The generality of our findings here summarized remains to be tested on related 2-oxoacid dehydrogenase complexes, both bacterial and human.

ASSOCIATED CONTENT

Supporting Information

Synthesis of [C2,C6′-^{13}C]ThDP and seven figures. This material is available free of charge via the Internet at http://pubs.acs.org.

AUTHOR INFORMATION

Corresponding Author

frjordan@rutgers.edu

Notes

The authors declare no competing financial interest.

ACKNOWLEDGMENTS

This work was supported at Rutgers by NIH-GM-050380 (to F.J.).

REFERENCES

(1) Koike, M.; Reed, L. J.; Carroll, W. R. *J. Biol. Chem.* **1960**, *235*, 1924.
(2) Stephens, P.; Darlison, M.; Lewis, H.; Guest, J. *Eur. J. Biochem.* **1983**, *133*, 155.
(3) Stephens, P.; Darlison, M.; Lewis, H.; Guest, J. *Eur. J. Biochem.* **1983**, *133*, 481.
(4) Stephens, P.; Lewis, H.; Darlison, M.; Guest, J. *Eur. J. Biochem.* **1983**, *135*, 519.
(5) Arjunan, P.; Sax, M.; Brunskill, A.; Chandrasekhar, K.; Nemeria, N.; Zhang, S.; Jordan, F.; Furey, W. *J. Biol. Chem.* **2006**, *281*, 15296.
(6) Nemeria, N.; Arjunan, P.; Brunskill, A.; Sheibani, F.; Wei, W.; Yan, Y.; Zhang, S.; Jordan, F.; Furey, W. *Biochemistry* **2002**, *41*, 15459.
(7) Kale, S.; Arjunan, P.; Furey, W.; Jordan, F. *J. Biol. Chem.* **2007**, *282*, 28106.
(8) Song, J.; Park, Y. H.; Nemeria, N. S.; Kale, S.; Kakalis, L.; Jordan, F. *J. Biol. Chem.* **2010**, *285*, 4680.
(9) Kale, S.; Ulas, G.; Song, J.; Brudvig, G. W.; Furey, W.; Jordan, F. *Proc. Natl. Acad. Sci. U.S.A.* **2008**, *105*, 1158.
(10) Kale, S.; Jordan, F. *J. Biol. Chem.* **2009**, *284*, 33122.
(11) Tittmann, K.; Golbik, R.; Uhlemann, K.; Khailova, L.; Schneider, G.; Patel, M.; Jordan, F.; Chipman, D. M.; Duggleby, R. G.; Hubner, G. *Biochemistry* **2003**, *42*, 7885.
(12) Seifert, F.; Ciszak, E.; Korotchkina, L.; Golbik, R.; Spinka, M.; Dominiak, P.; Sidhu, S.; Brauer, J.; Patel, M. S.; Tittmann, K. *Biochemistry* **2007**, *46*, 6277.
(13) Seifert, F.; Golbik, R.; Brauer, J.; Lilie, H.; Schroder-Tittmann, K.; Hinze, E.; Korotchkina, L. G.; Patel, M. S.; Tittmann, K. *Biochemistry* **2006**, *45*, 12775.
(14) Wei, W.; Li, H.; Nemeria, N.; Jordan, F. *Protein Expression Purif.* **2003**, *28*, 140.
(15) Yi, J.; Nemeria, N.; McNally, A.; Jordan, F.; Machado, R. S.; Guest, J. R. *J. Biol. Chem.* **1996**, *271*, 33192.
(16) Ali, S. T.; Guest, J. R. *Biochem. J.* **1990**, *271*, 139.
(17) Nemeria, N.; Volkov, A.; Brown, A.; Yi, J.; Zipper, L.; Guest, J. R.; Jordan, F. *Biochemistry* **1998**, *37*, 911.
(18) Nemeria, N.; Yan, Y.; Zhang, Z.; Brown, A. M.; Arjunan, P.; Furey, W.; Guest, J. R.; Jordan, F. *J. Biol. Chem.* **2001**, *276*, 45969.
(19) Holzer, H.; Schultz, G.; Villar-Palasi, C.; Juntgen-Sell, J. *Biochem. Z.* **1956**, *327*, 331.
(20) Jones, D. D.; Horne, H. J.; Reche, P. A.; Perham, R. N. *J. Mol. Biol.* **2000**, *295*, 289.
(21) Zhang, S., Rutgers, the State University of New Jersey, 2000.
(22) Kluger, R.; Tittmann, K. *Chem. Rev.* **2008**, *108*, 1797.
(23) Wille, G.; Meyer, D.; Steinmetz, A.; Hinze, E.; Golbik, R.; Tittmann, K. *Nat. Chem. Biol.* **2006**, *2*, 324.
(24) Tittmann, K.; Wille, G.; Golbik, R.; Weidner, A.; Ghisla, S.; Hubner, G. *Biochemistry* **2005**, *44*, 13291.
(25) Juan, E. C.; Hoque, M. M.; Hossain, M. T.; Yamamoto, T.; Imamura, S.; Suzuki, K.; Sekiguchi, T.; Takenaka, A. *Acta Crystallogr., Sect. F: Struct. Biol. Cryst. Commun.* **2007**, *63*, 900.
(26) Frey, P. A. *BioFactors* **1989**, *2*, 1.
(27) Zhang, S.; Zhou, L.; Nemeria, N.; Yan, Y.; Zhang, Z.; Zou, Y.; Jordan, F. *Biochemistry* **2005**, *44*, 2237.
(28) Gruys, K. J.; Datta, A.; Frey, P. A. *Biochemistry* **1989**, *28*, 9071.
(29) Flournoy, D. S.; Frey, P. A. *Biochemistry* **1986**, *25*, 6036.
(30) Pan, K.; Jordan, F. *Biochemistry* **1998**, *37*, 1357.
(31) Chiu, C. C.; Chung, A.; Barletta, G.; Jordan, F. *J. Am. Chem. Soc.* **1996**, *118*, 11026.
(32) Graham, L. D.; Packman, L. C.; Perham, R. N. *Biochemistry* **1989**, *28*, 1574.
(33) Jones, D. D.; Perham, R. N. *Biochem. J.* **2008**, *409*, 357.
(34) Jones, D. D.; Stott, K. M.; Reche, P. A.; Perham, R. N. *J. Mol. Biol.* **2001**, *305*, 49.
(35) Fries, M.; Stott, K. M.; Reynolds, S.; Perham, R. N. *J. Mol. Biol.* **2007**, *366*, 132.
(36) Zhang, S.; Liu, M.; Yan, Y.; Zhang, Z.; Jordan, F. *J. Biol. Chem.* **2004**, *279*, 54312.
(37) Cleland, W. W. *Biochemistry* **1975**, *14*, 3220.
(38) Fersht, A. *Structure and Mechanism in Protein Science: A Guide to Enzyme Catalysis and Protein Folding*; W. H. Freeman and Co.: New York, 1998; p 123.
(39) Jones, D. D.; Stott, K. M.; Howard, M. J.; Perham, R. N. *Biochemistry* **2000**, *39*, 8448.
(40) Berg, A.; Westphal, A. H.; Bosma, H. J.; de Kok, A. *Eur. J. Biochem.* **1998**, *252*, 45.

(41) Huhta, D. W.; Heckenthaler, T.; Alvarez, F. J.; Ermer, J.; Hubner, G.; Schellenberger, A.; Schowen, R. L. *Acta Chem. Scand.* **1992**, *46*, 778.
(42) Burbaum, J. J.; Raines, R. T.; Albery, W. J.; Knowles, J. R. *Biochemistry* **1989**, *28*, 9293.
(43) Perham, R. N. *Annu. Rev. Biochem.* **2000**, *69*, 961.
(44) Perham, R. N.; Jones, D. D.; Chauhan, H. J.; Howard, M. J. *Biochem. Soc. Trans.* **2002**, *30*, 47.
(45) Frank, R. A.; Price, A. J.; Northrop, F. D.; Perham, R. N.; Luisi, B. F. *J. Mol. Biol.* **2007**, *368*, 639.
(46) Frank, R. A. W.; Pratar, J. V.; Pei, X. Y.; Perham, R. N.; Luisi, B. F. *Structure* **2005**, *13*, 1119.
(47) Frank, R. A.; Titman, C. M.; Pratap, J. V.; Luisi, B. F.; Perham, R. N. *Science* **2004**, *306*, 872.
(48) Ciszak, E. M.; Korotchkina, L. G.; Dominiak, P. M.; Sidhu, S.; Patel, M. S. *J. Biol. Chem.* **2003**, *278*, 21240.
(49) Aevarsson, A.; Chuang, J. L.; Wynn, R. M.; Turley, S.; Chuang, D. T.; Hol, W. G. J. *Structure* **2000**, *8*, 277.
(50) Nakai, T.; Nakagawa, N.; Maoka, N.; Masui, R.; Kuramitsu, S.; Kamiya, N. *J. Mol. Biol.* **2004**, *337*, 1011.
(51) Wynn, R. M.; Kato, M.; Machius, M.; Chuang, J. L.; Li, J.; Tomchick, D. R.; Chuang, D. T. *Structure* **2004**, *12*, 2185.
(52) Machius, M.; Wynn, R. M.; Chuang, J. L.; Li, J.; Kluger, R.; Yu, D.; Tomchick, D. R.; Brautigam, C. A.; Chuang, D. T. *Structure* **2006**, *14*, 287.
(53) Kato, M.; Wynn, R. M.; Chuang, J. L.; Tso, S. C.; Machius, M.; Li, J.; Chuang, D. T. *Structure* **2008**, *16*, 1849.
(54) Pei, X. Y.; Titman, C. M.; Frank, R. A.; Leeper, F. J.; Luisi, B. F. *Structure* **2008**, *16*, 1860.
(55) Kern, D.; Kern, G.; Neef, H.; Tittmann, K.; Killenberg-Jabs, M.; Wikner, C.; Schneider, G.; Hubner, G. *Science* **1997**, *275*, 67.